# CHAPTER VI

## EXTENSIVE STUDY OF INCLUSION COMPLEXATION OF POTASSIUM SPARING DIURETIC AMILORIDE HYDROCHLORIDE WITH CYCLODEXTRIN MOLECULES BY MEANS OF ANTIMICROBIAL ASSAY

**Abstract:** Solubility development of supramolecular host-guest interaction between Amiloride hydrochloride with α and β-cyclodextrins were studied throughout this article. 1:1 host to guest stoichiometry of the inclusion complexation in the solution phase were confirmed by the Job's plot and further confirmation about the stoichiometry was also obtained from the mass spectra of the inclusion complexes. Association constants and thermodynamic parameter (ΔG) of the inclusion complexes were obtained using UV-vis spectroscopy. The mechanism of inclusion complexation was explored by 1H NMR spectroscopy. Furthermore, Density functional theory was employed to evaluate optimized geometries, adsorption energies, Non Covalent Interaction (NCI), electrostatic potential energy maps (ESP). The antimicrobial assay has also been done for the inclusion complexes.

**Keywords:** Cyclodextrins, Amiloride hydrochloride, Inclusion Complex, Binding constant, Antimicrobial activity, DFT.

**Introduction:**

Drugs play a significant role wherever they are used. In recent days drugs incorporated in cyclodextrins are of great concern because of its control release whenever it is within the cyclodextrin. A list of reports and other pharmacological applications are already there in the literature for the drug Amiloride hydrochloride **(Scheme 1)**. It is a guanidine diuretic and have moderate natriuretic and diuretic effects which means it has the capacity to excrete sodium through urine but sparing potassium, that is why it is also famous as 'potassium sparing diuretic'. No enzymatic basis was established for this action till now.

As the drug expels excess sodium from blood, automatically it reduces the blood pressure or any type of fluid withholding due to cardiac infarction. Amiloride also have some slight

non-postrual hypotensive effects. Chemically it is defined as 3,5-diamino-N-(diaminoethylene)-6-chloropyrazinecarboxamide, a synthetic pyrazine derivative.[1] It consists of a substituted pyrazine ring with an acylguanidine group attached to ring position 2, amino group attached at ring positions 3 and 5 , and a Cl group at position 6. Due to the presence of the guanidine moiety AMH is a weak base having $pk_a$ of 8.7 in aqueous solution but it is weakly soluble in water. Protonation of Amiloride occurs in the guanidine group, not in the amino group. In recent days drug delivery through buccal route is an additional way due to the advantage of larger surface area and great accessibility[2].

Because of having very low permeability and unpleasant taste buccoadhesive film is the smartest way to consume the drug AMH. Generally AMH is being consumed in the form of nano liposomal dry powder inhaler and liposomal formulation in spite of these privileges the drug seems to have major limitations e.g. the formulation may easily wash off from nose which requires a constant dose administration moreover the formulation is not stable enough to retain its composition in the body[2].

AMH also have side effects on the central nervous, gastrointestinal endocrine, musculoskeletal, dermatological and haematological systems and some common side effects are nausea, vomiting, diarrhoea and headache.

The rate of dissolution and poor aqueous solubility are the two important factors of a drug that affect its process of development, way of administration, its formulation and its mode of therapeutic application. It seems to be very difficult for poorly water-soluble drugs to administer through various routes.

There are several techniques to increase the solubility, dissolution property and bioavailability of the concerned drug but these techniques have some disadvantages too. Complexation through cyclodextrins can be used as a substitute and the process has already gained attention of many researchers and scientists in recent days.

As AMH is poorly water soluble, the major problem with this drug is its administration. Even though buccal route is the smartest way for administration of this drug but it has certain drawbacks which makes the drug fail to show its activity. Its controlled release to

the target site might be achieved by the formation of inclusion complex with cyclodextrins.

Generally cyclodextrins are of three types α, β and γ cyclodextrins **(Scheme 1).** They are naturally occurring oligosaccharides with 6, 7 and 8 glucopyranose units with hydrophobic interior cavity and hydrophilic outer surface. Among the three cyclodextrins β-cyclodextrin is the most preferable one for complexation because of its perfect size and diameter**[3].** We have chosen α and β- CD for our work. The main advantage of cyclodextrins is their water solubility, which permits non-covalent interactions (hydrogen bonding, van Der Waals forces of interactions etc.) with the drug or the guest concerned. After insertion of the guest molecule into cyclodextrin (either fully or partially) their physicochemical and biological properties are changed which leads to increase their bioavailability, solubility and applicability. Moreover, cyclodextrins are nontoxic and can cause complexation with very less toxicity.

Now in this study, incorporation of AMH into cyclodextrins has been done and it was observed that the complexes have enhanced antimicrobial activity than the pure drug.

## 2. EXPERIMENTAL SECTION

### 2.1. Materials

Amiloride hydrochloride, α and β-cyclodextrin, purity ≥98.0% and ≥97.0% were purchased from Sigma-Aldrich and were kept in a refrigerator as received to maintain the quality of the sample.

### 2.2. Apparatus

The Agilent 8453 UV-Visible Spectrophotometer was performed to record UV-vis spectra with an uncertainty of wavelength accuracy of ±0.5 nm. An automated digital thermostat, Julabo was used to control the cell temperature during experiments.

The data of HRMS spectra (of the solid ICs) were collected from a high-resolution quadrupole time-of-flight (Q-TOF) instrument having the feature of positive-mode electrospray ionization where the methanol solution of the solid ICs were used.

1H NMR spectra were recorded in $d_6$-DMSO solvent at 400 MHz in Bruker Avance instrument. The chemical shifts data, δ values are presented in parts per million.

### 2.3. Procedure

**2.3.1. Preparation Inclusion complexes:** Aqueous solution of AMH and CDs were prepared with triply distilled water. A digital analytical balance METTLER TOLEDO AG-285 was used weigh with an uncertainty of ±0.1 mg and loss of materials were avoided taking sufficient precautions. The equimolar aqueous solution of AMH and CDs were prepared separately. The solutions containing aqueous CDs in a beaker were placed on a hot top of a magnetic stirrer for stirring and the aqueous AMH solution was added dropwise to it. The solution containing CDs and AMH was allowed to stir for 10 hours maintaining temperature at 40-45°C. At last, the solution was suspended at 5 °C and was filtered to obtain white crystalline powder, which were then dried in air and preserved in vacuum desiccators.

**2.3.2. Computational Details:** All density functional theory (DFT) calculations are carried out using the Gaussian 16 program[4]. Geometry optimizations at ground state of the AMH, α-CD, β CD and inclusion complexes were carried out at M06-2X/6-31+G(d) level of theory. Different studies revealed that compared to other hybrid functionals, the M06-2X functional delivers reliable and precisely non-covalently bonded interaction energies (hydrogen bonding, π–π stacking)[5]. During optimization solvent effects (water) were introduced by applying the Polarizable Continuum Model (PCM)[6] using the integral equation formalism variant. Vibration frequency calculations (no imaginary frequency) were obtained at the same level of theory to verify whether the optimized geometry resides to the minima on the potential energy surfaces. To interpret weak interactions like H-bonding, van der Waals interactions, steric interactions Non-Covalent Interaction (NCI) index plots of the reduced density gradient (RDG or s) were obtained using the Multiwfn 3.7 suite[7] at their corresponding ground state geometries. Finally, utilizing the following formula, adsorption energies or binding energies ($\Delta E_{ads}$) of the composite systems were calculated:

$$\Delta E_{ads} = E_{AMH\text{-}CD} - E_{AMH-\ ECD}$$

Where $E_{AMH-CD}$, $E_{AMH}$, $E_{CD}$ are the total energy of the geometry optimized complexes, AMH and the CD molecules, respectively.

**2.3.3. Antimicrobial activity:** Disk diffusion method was followed for viewing the antibacterial activity of synthesized test samples [Drug, IC-1, IC-2, DMSO corresponds to A(ii), B(iii), C(iv) and D(i) respectively] under study. Against three strains of gram positive bacteria (Bacillus subtilis ATCC 11774, Bacillus megaterium ATCC 14581 and Staphylococcus aureus ATCC 11632) and two strains of gram negative bacteria (Salmonella typhimurium ATCC25241and Escherichia coli ATCC 11229) antibacterial activity was assessed with seven different concentrations of each of the test samples (25, 50, 100, 200, 300, 400, 500 µg/ml). The microbes were cultured for 6 hrs on nutrient broth before their application to obtain rapidly growing healthy feasible cells. Nutrient agar plate was prepared by uniform mixing of 100 µl test organism with 15 ml sterilized nutrient agar through the process of solidification by cooling under laminar airflow. After 30 min of mixing paper disk soaked with appropriate concentration of test solution was placed in the nutrient agar plate. The zone of inhibition was calculated in the scale bar of millimeter calibration after 24 h of incubation at 37 °C.

## 3. Result and discussion

### 3.1 Job plot: the host – guest stoichiometry in inclusion complex:

As the molecular recognition of a guest molecule into the cavity of host molecule depends on the size of the guest molecule and the cavity volume of the host molecule, it is vital to determine the host to guest ratio in the inclusion complex i.e. the stoichiometry of the inclusion complex. Here, we employed the great Job's method[8], using UV-vis spectroscopic data to determine the stoichiometry of the host-guest inclusion complexes. A set of solutions of mole fraction ranging from 0 to 1 were prepared by mixing aqueous AMH and CDs and recorded the spectra at 298.15 K of temperature. The absorbance at λmax = 364 nm were considered for the calculation **(Figure 1).** The value of R, at the maxima of ΔA×R vs R plot, signifies the stoichiometry of inclusion complexes. Where, ΔA represents the differences in absorbance between pure AMH and each of the solutions of the set **(Table S1, S2 and Figure 1).** R indicates [CDs]/[AMH]+[CDs] and its value of R =

0.33, 0.5, 0.66 corresponding to the maxima recommends the 1:2, 1:1 and 2:1 host to guest stoichiometry in the inclusion complexes[9]. In case of our present work we found the maxima at R = 0.5 indicating 1:1 host to guest stoichiometry in the inclusion complexes[10] **(Scheme 2)**.

**3.2 HRMS: The confirmation about the stoichiometry of the Inclusion complexes:**

The molecular ion peak with an appreciable intensity at the m/z ratio corresponding to the molar mass of a host molecule added to the same of the guest molecule in the HRMS spectra is actually a great evidence for saying about the host-guest stoichiometry of the inclusion complex. The HRMS spectra of the prepared inclusion complexes were recorded after dissolving these in methanol. The spectra, shown in the **Figure 2 and 3**, have the molecular ion peaks at the m/z 1202.9025 and 1365.0427 correspond to the $[AMH+\alpha\text{-}CD+H]^+$ and $[AMH+\beta\text{-}CD+H]^+$ respectively, signify the formation of [AMH + α-CD] and [AMH + β-CD] inclusion complexes of 1:1 host to guest stoichiometry must have an appreciable stability of the molecular assembly formed[11],[12] (Scheme 2).

**3.3 1H NMR spectral analysis:**

The mechanism of inclusion complexation i.e. the identification of part of the guest molecule most probably the hydrophobic part that undergoes insertion into the hydrophobic cavity of cyclodextrin and the extent to which it get inserted into the hydrophobic cavity of cyclodextrin is yet to be explored. Here, 1H NMR spectra analysis appeared as the great technique to explore the same with a pronounced fulfilment.

Because of the truncated structure of cyclodextrins, H3 and H5 protons are oriented inside the cavity whereas H1, H2 and H4 protons are exposed to the outer side of CDs[13] (Figure.4). That's why, H3 and H5 protons of CDs would experience an interaction with the guest molecule undergoing insertion into the cavity of CDs and register a chemical shift in 1H NMR spectrum due to their mutual shielding through space[14]. Here the encapsulated aromatic moiety of the AMH, having ring current exerts diamagnetic shielding to the H3 and H5 protons of the CDs[15] **(Figure 4)**.

Here, the experiment goes through our expectation and it reflected in the same when we analyse the 1H NMR spectra of pure α-CD, β-CD, AMH as well as the inclusion complexes

are shown in **Figure 5 and 6**. The considerable upfield shift of the H3, H5 protons of CDs in the 1H NMR spectra confirms the formation of inclusion complexes.[16]

### 3.4 Ultraviolet Spectroscopy: The stability of the Inclusion Complexes:

The binding energy of the inclusion complexes formed in solution phase, saying about the stability of the inclusion complexes was calculated by employing well-known Benesi-Hildebrand equation[17],[18] and using UV-vis spectroscopic data. In the aqueous solution of cyclodextrin, the hydrophobic cavity of cyclodextrin being less polar compared to aqueous environment must have lower molar extinction coefficients (Δε) than that of the aqueous environment. This is why, we expected the absorbance of the guest molecule must change while going from polar aqueous media to the apolar hydrophobic cavity of the CDs to form ICs[19],[20] and we observed the same trend in absorbance which are shown in **Figure 7**. The UV-vis spectroscopic data **(Figure S3 and S4)** were fed into the following Benesi-Hildebrand equation (1) and the calculated values are listed in the **Table 1**.

$$\frac{1}{\Delta A} = \frac{1}{\Delta\varepsilon[AMH]K_a}\frac{1}{[CD]^n} + \frac{1}{\Delta\varepsilon[AMH]} \qquad (1)$$

Where, ΔA is the difference in absorbances of AMH without CDs and with the CDs. [AMH] represents the concentration of AMH. The value of (n) says about the stoichiometry of the ICs. When the linearity of the double reciprocal plot fits by putting n=1 in the above equation then it suggests 1:1 stoichiometry of the ICs. But, when n=2 suggests the 2:1 inclusion complex of the Host to the Guest[21]. Here, we observed a linear relationship of the Benesi-Hildebrand double reciprocal plot, considering n=1, indicating the composition of complex was 1:1.

The binding constant (Ka) of the inclusion complexes were calculated from the obtainable values of intercepts and slopes of the Benesi-Hildebrand double reciprocal plot **(Figure 7)** and are listed in the **Table 1.**

The binding constants of the inclusion complexes so obtained were fed into equation (2) and the change in free energy of the inclusion process were listed in the **Table 1**.

$$\Delta G = -RTlnK_a \qquad (2)$$

### 3.5 Theoretical study of the interaction in the inclusion complexes:

Optimized geometries of the AMH+α-CD and AMH+β-CD inclusion complexes are shown in **Figure 8**. In the relaxed geometry of the AMH+β-CD composites AMH occupies in the centre of the cavity indicating complete encapsulation by β-CD. On the other hand in AMH+α-CD due to the smaller radius of α-CD AMH is partially encapsulated. The higher affinity of AMH of AMH by β-CD has been confirmed by the strong H-bonds ranging from 1.94 Å to 2.93 Å which is short compared to the H- bonds in AMH+α-CD. The stronger Hydrogen bonding between –NH2 groups of AMH and –OH group of β-CD in AMH+β-CD accounts the large adsorption energy of -5.52eV which is high compared to AMH+α-CD ($E_{ads}$ =-4.51 eV) in aqueous medium.

To account different weak interactions operating between AMH and α-CD, β-CD we have analysed the RDG plots as shown in the **Figure 9**. A large scattered points in the region --0.03-0.04 of the RDG plot revealed that predominant H-bonding interaction is operating between AMH and β-CD units while due to the partial inclusion this interaction is weaker in AMH+α-CD.

### 3.6 Antimicrobial activity:

All the synthesized samples except the solvent **DMSO (i)** displayed potent antimicrobial activity against both gram positive and gram negative bacteria as apparent by measuring the diameter of zone of inhibition **(Figure 10 and Table S5)**. In comparison to all the studied samples, quantitative measurement of inhibition zone in millimeter scale indicates that at uppermost (100 µg/ml) and lower most concentration (25 µg/ml) best activity was displayed by test **sample (iii)** (combination of α-Cyclodextrin and Amiloride hydrochloride) against both gram positive and gram negative bacteria, Escherichia coli with inhibitory zone of 25.33 ± 1.528 mm and 14 ± 1.732 mm respectively. Beside this **sample (iii)** at any used concentration displayed prominent zone of inhibition against both gram positive and gram negative microbes[22] reported bacteriostatic activity of amiloride against different strains of bacteria at concentration range of 25 to 1,300 µg /ml. The concentration range of **sample (iii)** used for antimicrobial activity in the present study lies within the above mentioned range. **Amiloride HCl, Sample (ii)** was also reported to display antimicrobacterial activity when used in combination with rifampicin[23]. Cyclodextrin was reported to appropriately control the drug release rate

of its conjugated antimicrobial component and thereby display effective antimicrobial activity[24]. Conjugation of α-Cyclodextrin with Moringin displayed potent antimicrobial activity against Staphylococcus aureus[25]. Similarly the antibacterial activity of essential oils extracted from Prostanthera increases by two to four fold when encapsulated with α-cyclodextrin[26]. In the present study conjugation of amiloride hydrochloride with α-Cyclodextrin showed better antimicrobial activity than amiloride hydrochloride alone probably due to better drug release kinetics of α-Cyclodextrin. Beside this, current study reports better antimicrobial activity of amiloride hydrochloride when conjugated with α-Cyclodextrin [**sample (iii)]** than β-Cyclodextrin [**sample (iv)]**. This finding contradicts with the finding of which reported better activity of β-Cyclodextrin than α-Cyclodextrin against Staphylococcus aureus and Escherichia coli when Complexes with Trans-Cinnamaldehyde[27]. Such contradict observation was probably because different drugs behaves differently with Cyclodextrin. Probably amiloride HCl showed better complex formation kinetics with α-Cyclodextrin [**sample (iii)]** than β-Cyclodextrin [**sample (iv)]** and thereby displaying better synergistic antimicrobial activity when conjugated with α-Cyclodextrin [**sample (iii)]**. At minimum tested concentration (25 µg/ml) sample A and C was found to be more effective against gram positive bacteria than gram negative bacteria. While **sample (i)**, failed to displayed any bactericidal activity at any of the used concentrations. This observation was supported by the observation of **Carlos de Brito et al. (2017)** which stated that concentrations of DMSO do not interfere with the viability of the bacterial strains.

Among the tested gram positive bacteria, sample **Drug (ii), IC-1 (iii) and IC-2 (iv)** was found to be effective at any used concentration against Bacillus subtilis. While **sample (ii)** and **(iv)** was found to be effective against Bacillus megaterium and Staphylococcus aureus at concentration of 100µg/ml, below which no activity was noted. The probable reason for this type of activity may be that at low concentration thick peptidoglycan layer, consisting of linear polysaccharide chains cross linked by short peptides makes the membrane wall of gram positive bacteria a rigid and compact structure which creates difficulty for silver nanoparticles to penetrate the bacterial cell wall[28]. Against gram negative bacteria Salmonella typhimurium **Sample (ii)** showed bactericidal activity at maximum concentration of 100µg/ml while **sample (iii)** displayed the activity from the concentration range of 50µg/ml. On the other side against Escherichia coli **sample (ii)**

showed better activity than **sample (iv)**. All the three bactericidal samples (viz. ii, iii and iv) showed better antimicrobial activity against gram positive bacteria than gram negative bacteria this is probably because thin peptidoglycan layer in the cell wall of gram negative bacteria allows easy penetration of the test samples damaging cellular and metabolic processes causing bacterial death[29].

## 4. Conclusions:

All the experiments suggest the successful formation of inclusion complex with 1:1 stoichiometry. The association constants of the inclusion complexes of AMH formed with β-cyclodextrin were found greater than that of the inclusion complexes formed with the α-cyclodextrin and hence more stable, this is may be due to the better fitness of the guest molecule into the larger hydrophobic cavity of β-cyclodextrin compared to the α-cyclodextrin. Furthermore analysis of adsorption energies, ESP, HOMO , LUMO distributions revealed that compared to AMH/α-CD , AMH/β-CD is quite stable and possesses significant amount of donor (guest ) – acceptor (host) charge transfer interactions. Asymmetry in ESP maps suggests enhanced solubility of AMH/β-CD over the AMH/α-CD inclusion complexes. The ready availability of the association constants enables us to calculate the thermodynamic parameter(ΔG) of the inclusion process which makes the thermodynamic ground of the approach and recognise it as a thermodynamically viable process. The antimicrobial activity of the drug was seemed to be enhancing after inclusion especially with α-CD, which is complementary with the findings from association constants, i.e. more association constant less free the drug. Thus, the hydrophobic-hydrophobic interaction would become the driving forces for the formation of inclusion complexes.

**Conflicts of interest:** There are no conflicts of interest.

**Acknowledgements:** Prof. M. N. Roy would like to acknowledge UGC, New Delhi, Government of India, for being awarded One Time Grant under Basic Scientific Research (BSR) for augmenting innovative research in the field of Chemical Sciences via the grant-in-Aid no. F.4-10/2010 (BSR).

## TABLES

**Table 1:** Association Constants obtained from Benesi-Hildebrand method ($K_a$) and change in free energy (ΔG).

| Inclusion complexes | Binding constants ($K_a/M^{-1}$)×$10^3$ | Free energy change (ΔG) ($kJ/M^{-1}$) |
|---|---|---|
| AMH+α-CD | 5.66 | -21.93 |
| AMH+β-CD | 6.93 | -21.42 |

**Table S1**. UV-Vis spectroscopic data for the generation of Job plots of aqueous AMH+*α*-CD system at 298.15 K[a].

| AMH + α - CYCLODEXTRIN | | | | | | | |
|---|---|---|---|---|---|---|---|
| AMH (mL) | α-CD (mL) | AMH (μM) | α-CD (μM) | $\frac{[AMH]}{[AMH]+[\alpha-CD]}$ | Absorbance (A) | ΔA | $\frac{\Delta A \times [AMH]}{[AMH]+[\alpha-CD]}$ |
| 0 | 3 | 0 | 100 | 0 | 1.5203 | 1.5115 | 0.0000 |
| 0.3 | 2.7 | 10 | 90 | 0.1 | 1.3759 | 1.3759 | 0.1376 |
| 0.6 | 2.4 | 20 | 80 | 0.2 | 1.2276 | 1.2276 | 0.2455 |
| 0.9 | 2.1 | 30 | 70 | 0.3 | 1.0793 | 1.0793 | 0.3238 |
| 1.2 | 1.8 | 40 | 60 | 0.4 | 0.9343 | 0.9343 | 0.3737 |
| 1.5 | 1.5 | 50 | 50 | 0.5 | 0.7695 | 0.7695 | 0.3847 |
| 1.8 | 1.2 | 60 | 40 | 0.6 | 0.6221 | 0.6221 | 0.3733 |
| 2.1 | 0.9 | 70 | 30 | 0.7 | 0.4792 | 0.4792 | 0.3354 |
| 2.4 | 0.6 | 80 | 20 | 0.8 | 0.2930 | 0.2930 | 0.2344 |
| 2.7 | 0.3 | 90 | 10 | 0.9 | 0.1816 | 0.1816 | 0.1635 |
| 3 | 0 | 100 | 0 | 1 | 0.0088 | 0.0088 | 0.0088 |

[a]Standard uncertainties in temperature *u* are: *u*(T) = ±0.01 K.

**Table S2**. UV-Vis spectroscopic data for the generation of Job plots of aqueous AMH+$\beta$-CD system at 298.15 K[a].

| AMH + β - CYCLODEXTRIN | | | | | | | |
|---|---|---|---|---|---|---|---|
| **AMH (mL)** | **$\beta$-CD (mL)** | **AMH (µM)** | **$\beta$-CD (µM)** | $\frac{[AMH]}{[AMH]+[\beta-CD]}$ | **Absorbance (A)** | **ΔA** | $\frac{\Delta A \times [AMH]}{[AMH]+[\beta-CD]}$ |
| 0 | 3 | 0 | 100 | 0 | 1.5818 | 1.5721 | 0.0000 |
| 0.3 | 2.7 | 10 | 90 | 0.1 | 1.4080 | 1.4080 | 0.1408 |
| 0.6 | 2.4 | 20 | 80 | 0.2 | 1.2566 | 1.2566 | 0.2513 |
| 0.9 | 2.1 | 30 | 70 | 0.3 | 1.1105 | 1.1105 | 0.3332 |
| 1.2 | 1.8 | 40 | 60 | 0.4 | 0.9532 | 0.9532 | 0.3813 |
| 1.5 | 1.5 | 50 | 50 | 0.5 | 0.7977 | 0.7977 | 0.3989 |
| 1.8 | 1.2 | 60 | 40 | 0.6 | 0.6441 | 0.6441 | 0.3864 |
| 2.1 | 0.9 | 70 | 30 | 0.7 | 0.4749 | 0.4749 | 0.3324 |
| 2.4 | 0.6 | 80 | 20 | 0.8 | 0.3221 | 0.3221 | 0.2577 |
| 2.7 | 0.3 | 90 | 10 | 0.9 | 0.1812 | 0.1812 | 0.1631 |
| 3 | 0 | 100 | 0 | 1 | 0.0097 | 0.0097 | 0.0097 |

**Table S3**. UV-vis spectroscopic data for the Benesi-Hildebrand double reciprocal plot of (AMH+α-CD) system at 298.15K

| **Temp (K[a])** | **AMH (µM)** | **α-CD (µM)** | **Ao** | **A** | **ΔA** | **1/[α-CD] ($M^{-1}$)** | **1/ΔA** | **Intercept** | **Slope** | **Ka ($M^{-1}\times10^3$)** |
|---|---|---|---|---|---|---|---|---|---|---|
| 298.15 | 35 | 25 | 0.5620 | 0.6042 | 0.0422 | 0.0400 | 23.6831 | 2.9815 | 527.18 | 5.66 |
| | 35 | 30 | | 0.6098 | 0.0479 | 0.0333 | 20.8973 | | | |
| | 35 | 35 | | 0.6171 | 0.0551 | 0.0286 | 18.1501 | | | |
| | 35 | 40 | | 0.6208 | 0.0588 | 0.0250 | 17.0107 | | | |
| | 35 | 45 | | 0.6345 | 0.0726 | 0.0222 | 13.7822 | | | |

**Table S4**. UV-vis spectroscopic data for the Benesi-Hildebrand double reciprocal plot of (AMH+ β-CD) system at 298.15K

| Temp ($K^a$) | AMH (μM) | β-CD (μM) | Ao | A | ΔA | 1/[ β - CD] ($M^{-1}$) | 1/ΔA | Intercept | Slope | Ka ($M^{-1}\times10^3$) |
|---|---|---|---|---|---|---|---|---|---|---|
| 298.15 | 35 | 25 | 0.5620 | 0.6053 | 0.0433 | 0.0400 | 23.0818 | 3.4689 | 500.37 | 6.93 |
| | 35 | 30 | | 0.6107 | 0.0488 | 0.0333 | 20.5115 | | | |
| | 35 | 35 | | 0.6179 | 0.0559 | 0.0286 | 17.8903 | | | |
| | 35 | 40 | | 0.6215 | 0.0595 | 0.0250 | 16.8106 | | | |
| | 35 | 45 | | 0.6351 | 0.0732 | 0.0222 | 13.6691 | | | |

**Table S5:** Antimicrobial activity of drug, IC-1, IC-2 and solvent DMSO sample name against tested microorganisms. Results are expressed as Mean ± SD of triplicate determinations.

| | | Zone of Inhibition (mm) | | |
|---|---|---|---|---|
| **Microorganisms** | **Sample ID** | **25 μg/ml** | **50 μg/ml** | **100 μg/ml** |
| ***B Subtilis*** | (ii) | 8.33 ± 2.52 | 14.33 ± 0.577 | 18.33 ± 1.523 |
| | (iii) | 5.33 ± 0.577 | 12.33 ± 0.577 | 18.67 ± 1.155 |
| | (iv) | 5.66 ± 0.577 | 9.33 ± 0.577 | 16.67 ± 0.577 |
| | (i) | 0 | 0 | 0 |
| ***B megaterium*** | (ii) | 0 | 0 | 14.33 ± 1.153 |
| | (iii) | 7.33 ± 0.577 | 10.67 ± 1.15 | 20.33 ± 0.577 |
| | (iv) | 0 | 0 | 12.33 ± 0.577 |
| | (i) | 0 | 0 | 0 |
| ***S aureus*** | (ii) | 0 | 0 | 11.33 ± 1.15 |
| | (iii) | 6.66 ± 0.577 | 13.33 ± 1.15 | 21.67 ± 2.08 |
| | (iv) | 0 | 0 | 10.67 ± 0.577 |
| | (i) | 0 | 0 | 0 |
| ***S typhimurium*** | (ii) | 0 | 0 | 10.67 ± 0.577 |
| | (iii) | 8 ± 1.732 | 14.67 ± 2.082 | 21.67 ± 2.082 |
| | (iv) | 0 | 6.33 ± 0.577 | 7.33 ± 0.577 |
| | (i) | 0 | 0 | 0 |
| ***E Coli*** | (ii) | 6.66 ± 0.577 | 12.33 ± 1.155 | 18 ± 1 |
| | (iii) | 14 ± 1.732 | 20.67 ± 0.577 | 25.33 ± 1.528 |
| | (iv) | 0 | 16 ± 2 | 21.33 ± 0.577 |
| | (i) | 0 | 0 | 0 |

**FIGURES**

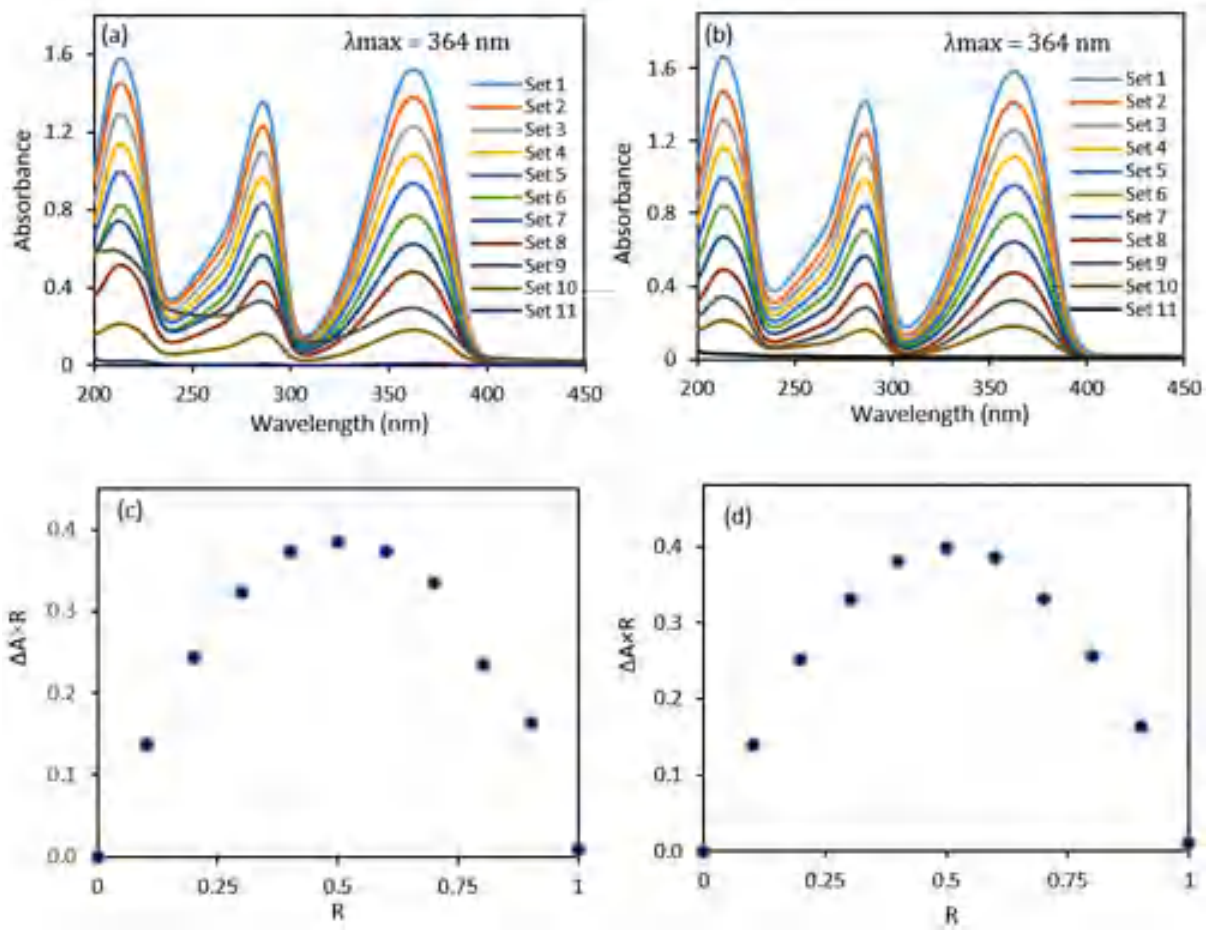


**Figure 1 (a,b,c,d):** UV-vis spectra for the generation of Job plots of (a) AMH+α-CD and (b) AMH+β-CD systems and Job Plots of (c) AMH+α-CD and (d) AMH+β-CD systems at  = 364 nm.

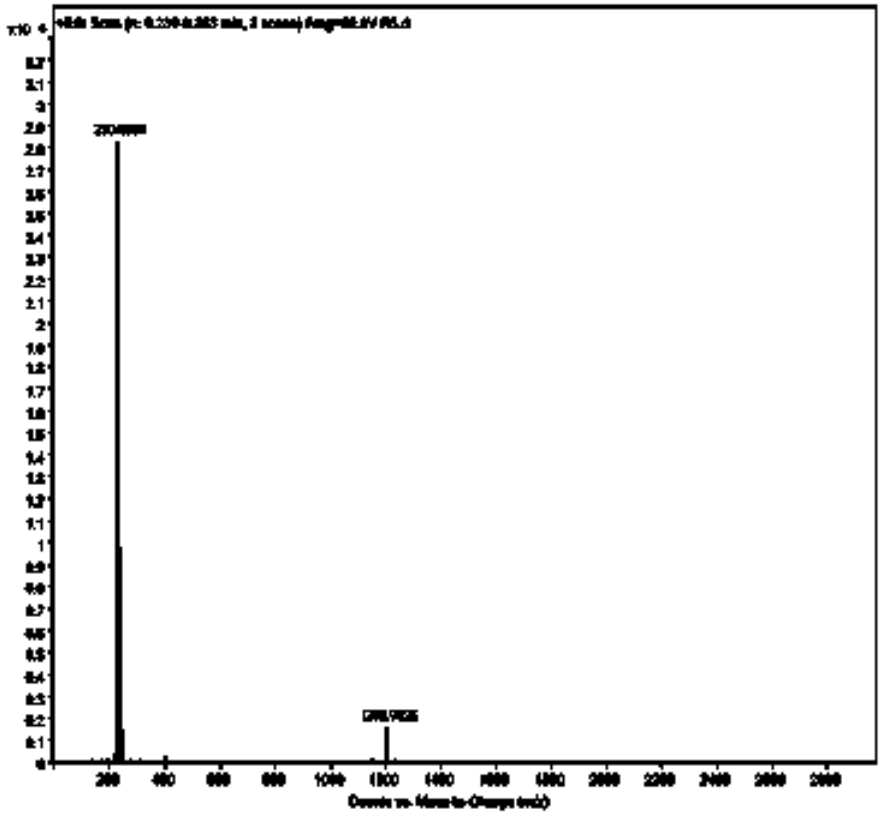

**Figure 2:** HRMS spectra of the AMH+α-CD Inclusion complex.

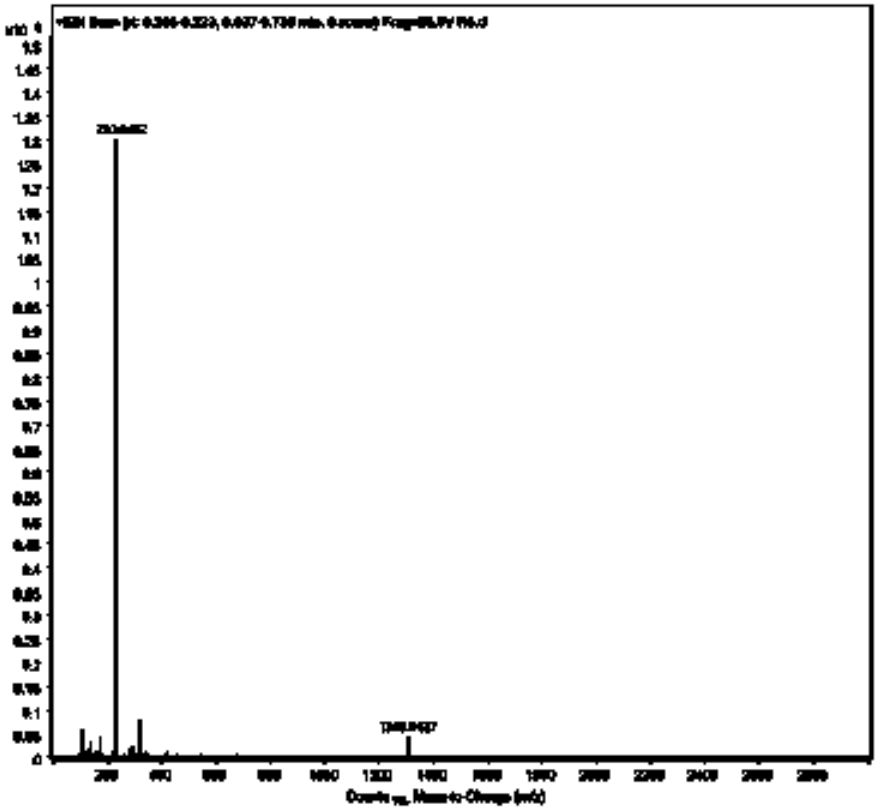

**Figure 3:** HRMS spectra of the AMH+β-CD Inclusion Complex.

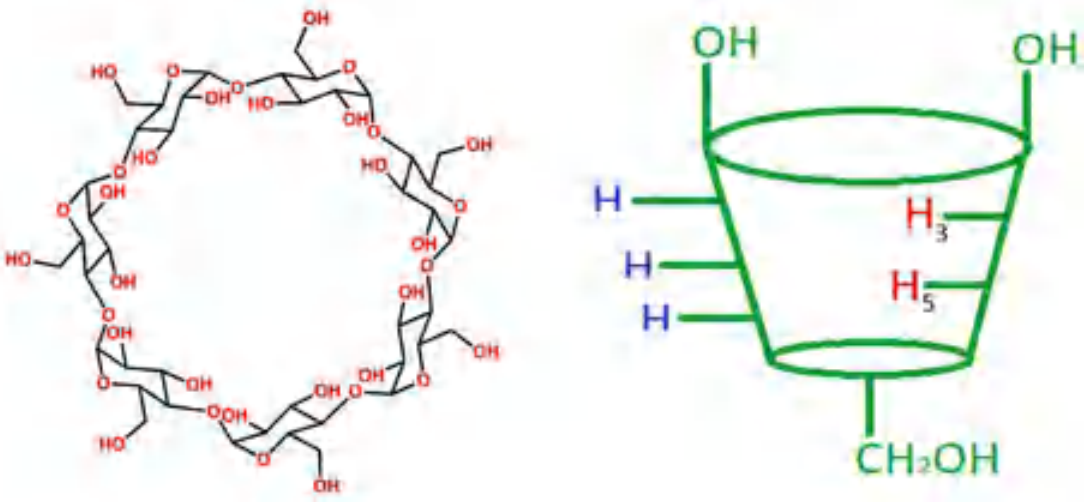


**Figure 4:** Truncated structure of Cyclodextrins showing $H_3$ and $H_5$ protons of Cyclodextrins.

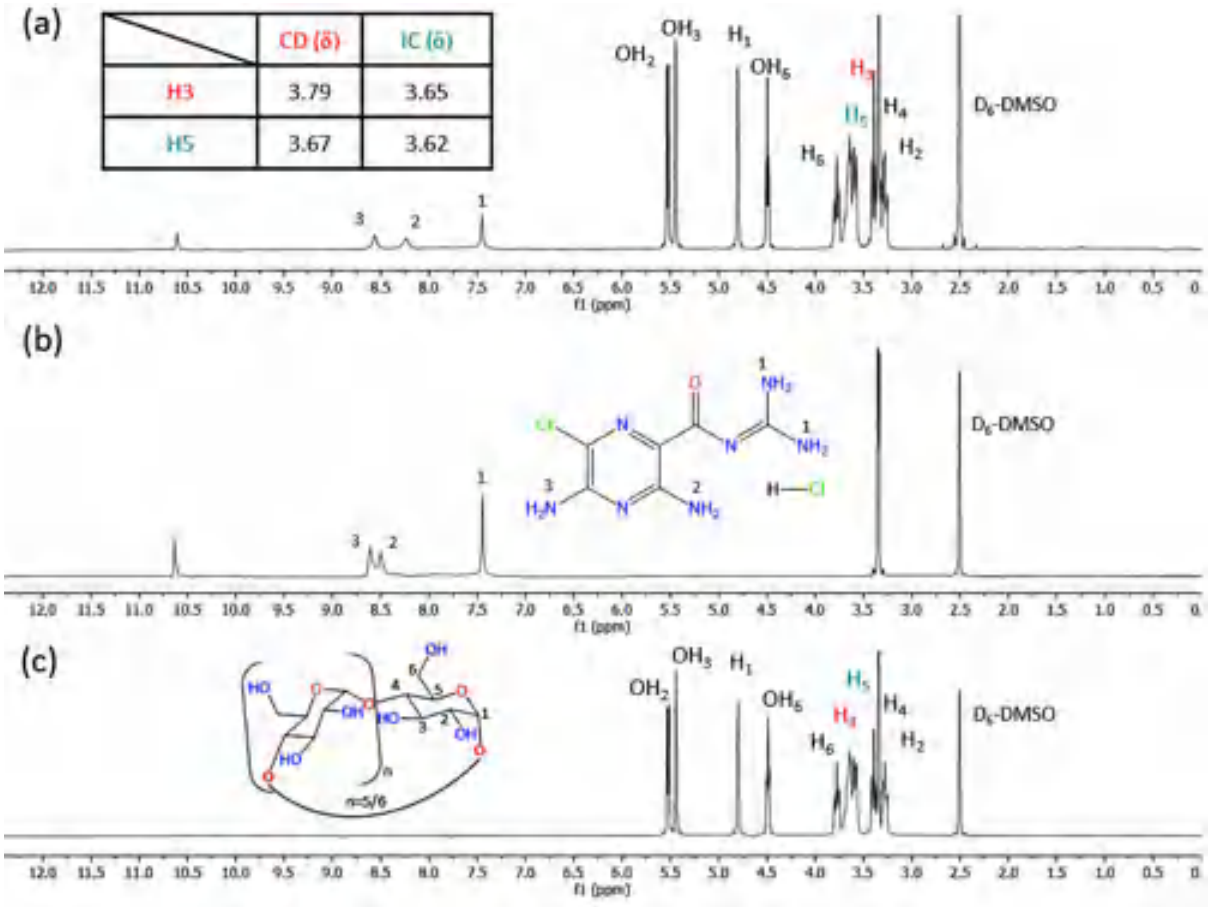


**Figure 5(a,b,c):** 1H NMR spectra of (a) AMH+α-CD Inclusion complex,(b) AMH and (c) α-CD

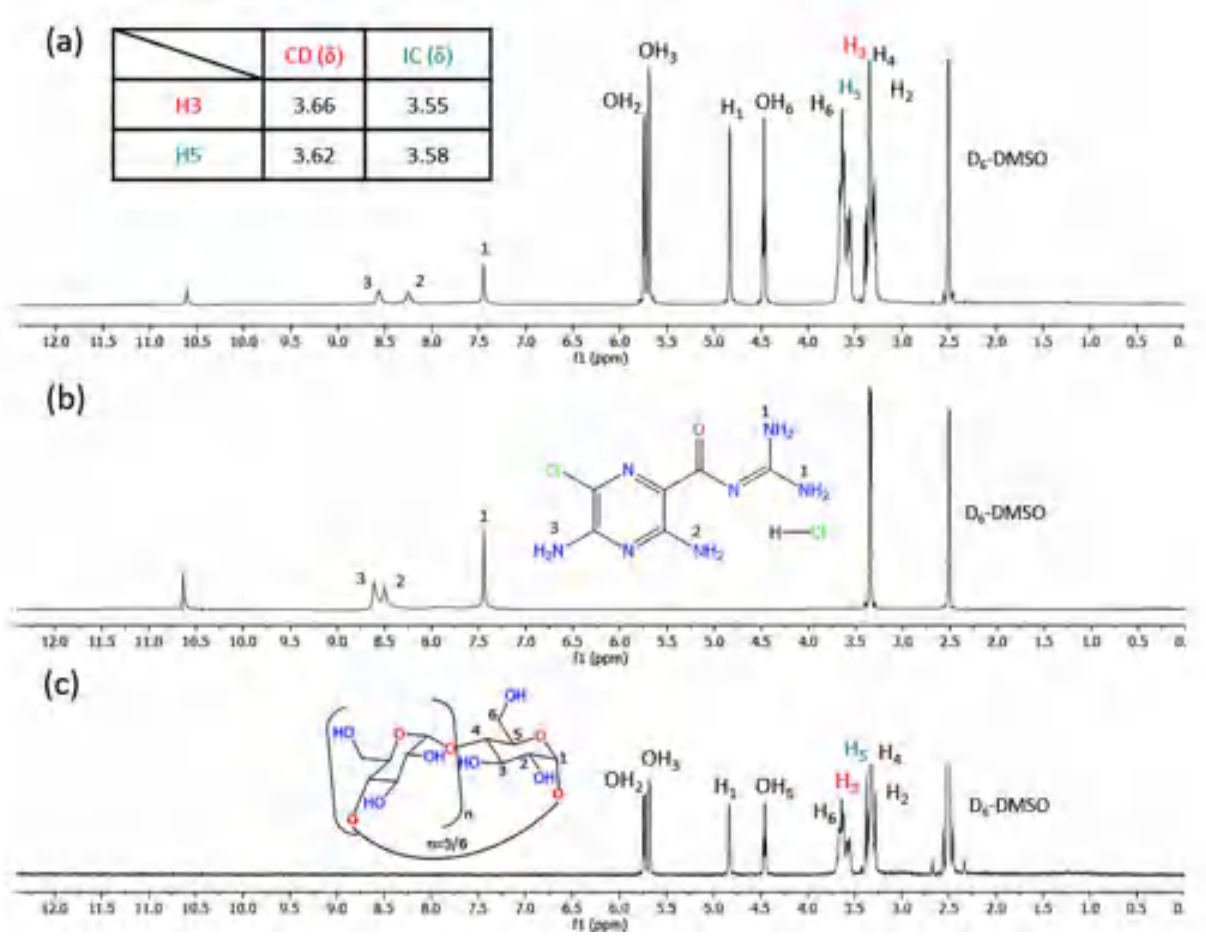


**Figure 6(a,b,c):** 1H NMR spectra of (a) AMH+β-CD Inclusion complex, (b) AMH and (c) β-CD.

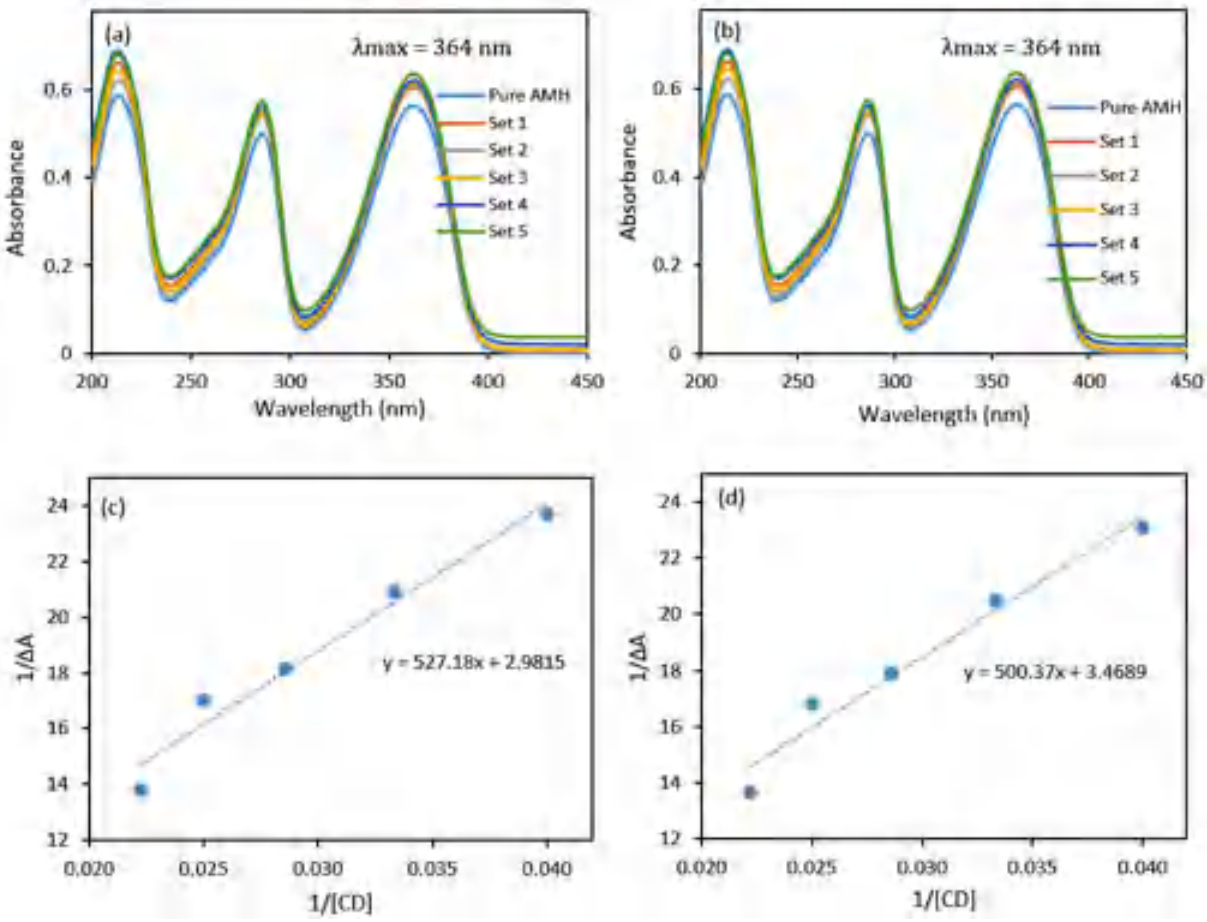


**Figure 7(a,b,c,d):** UV visible spectra (a) AMH+α-CD, (b) AMH+β-CD) systems for the generation of Benesi Hildebrand double reciprocal plots of (c) AMH+α-CD, (d) AMH+β-CD systems at 298.15K.

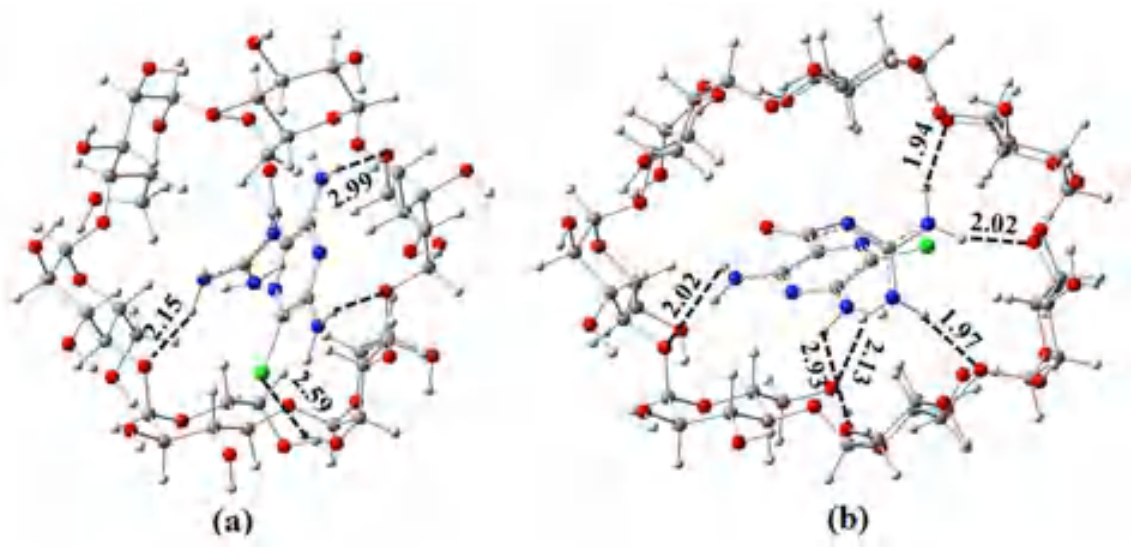


**Figure 8:** Optimized geometries for the (a) AMH+α-CD (b) AMH+β-CD composite at M06-2X/6-31+G(d) level of theory. Red, gray, white, blue color represent oxygen, carbon, hydrogen, nitrogen atoms respectively.

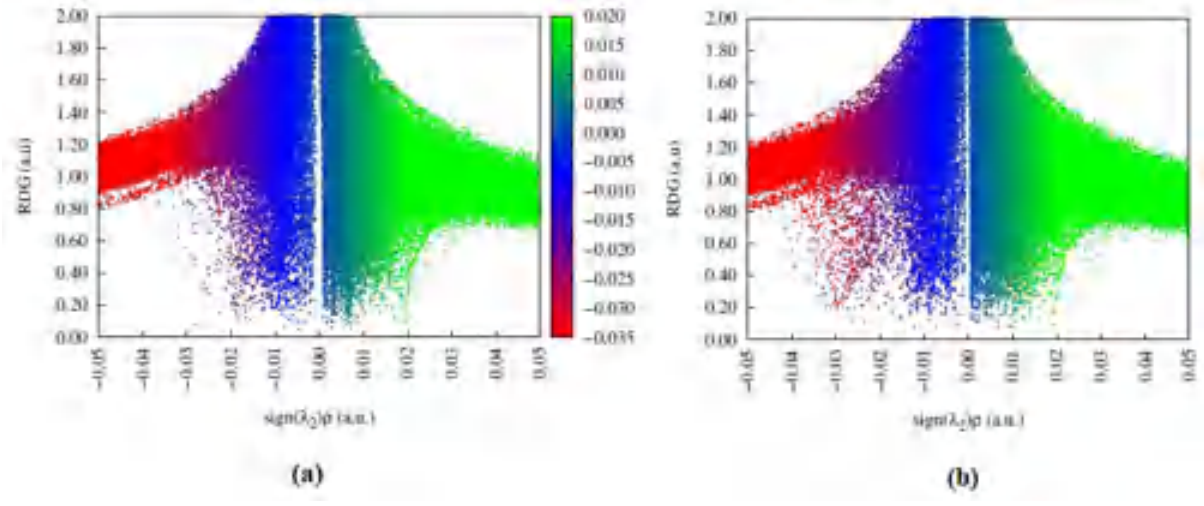


**Figure 9:** Plots of reduced density gradient (RDG) for (a) AMH+α-CD and (b) AMH+β-CD inclusion complexes.

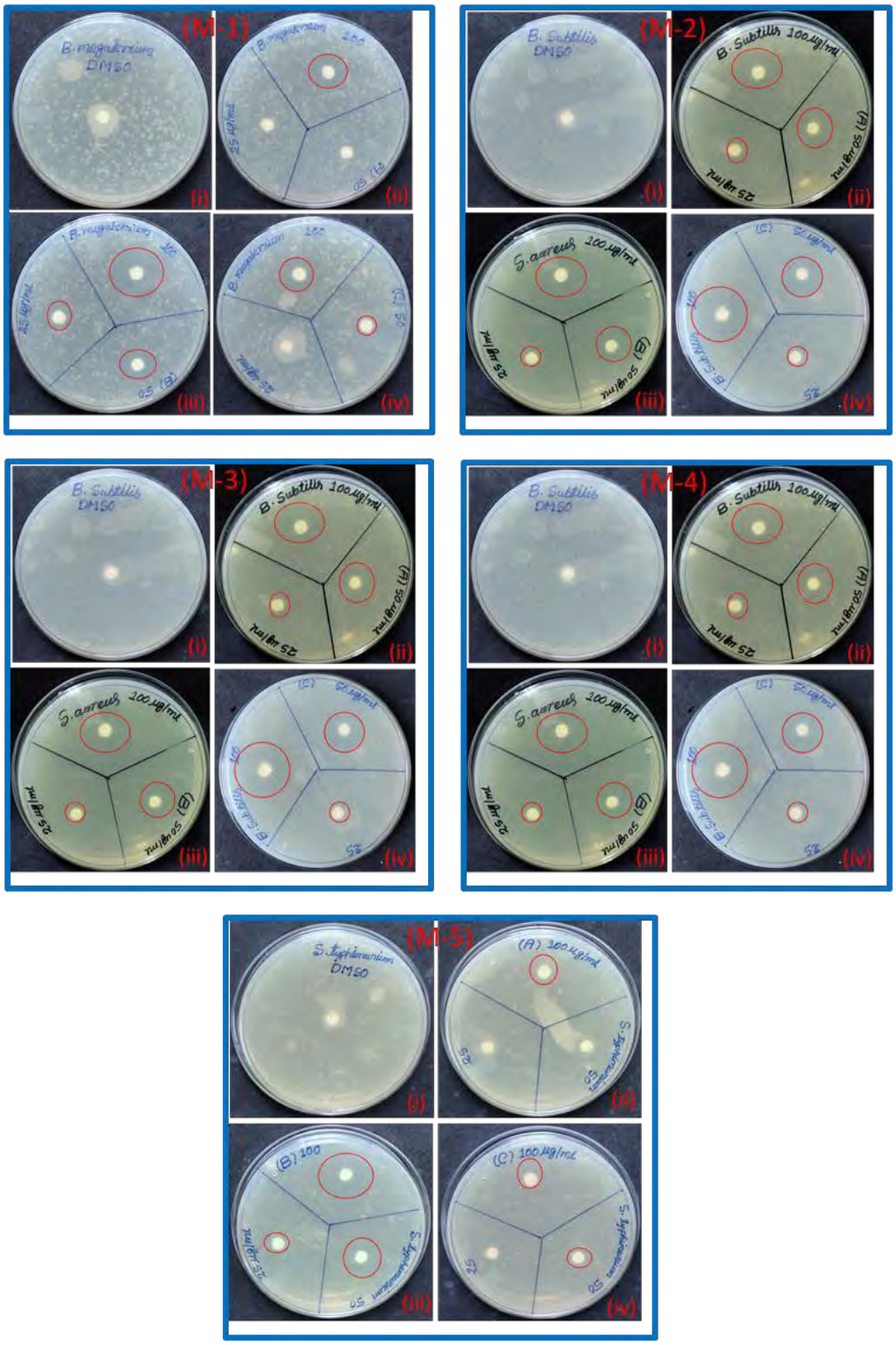


**Figure 10(M-1, M-2, M-3, M-4, M-5):** Antimicrobial activity of (i) DMSO, (ii) AMH, (iii) AMH+α-CD Inclusion complex, (iv) AMH+β-CD Inclusion complex against test organisms viz. **(M-1)** *B megaterium,* **(M-2)** *B Subtilis,* **(M-3)** *E Coli,* **(M-4)** *S aureus*, **(M-5)** *S typhimurium*. Antimicrobial potentiality was assessed at three different concentrations of each of the samples, viz. 100 µg/mL, 50 µg/mL and 25 µg/mL.

**SCHEMES**

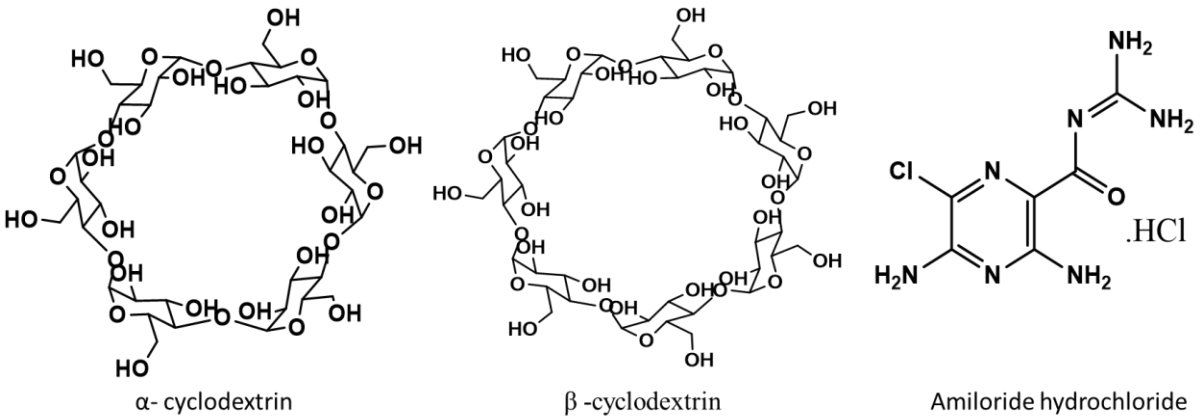


**Scheme 1:** Molecular structures of α–cyclodextrin, β-Cyclodextrin and Amiloride hydrochloride.

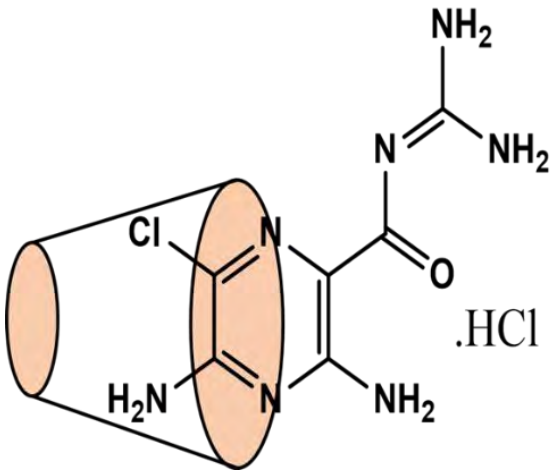

**Scheme 2:** Formation of Inclusion complex through the wider rim of the cyclodextrin.